


Article

A Neural Network-Based Four Phases Interleaved Boost Converter for Fuel Cell System Applications

El Manaa Barhoumi ^{1,2,*}, Ikram Ben Belgacem ³, Abla Khiareddine ⁴, Manaf Zghaibeh ¹ and Iskander Tlili ⁵

¹ Department of Electrical and Computer Engineering, College of Engineering, Dhofar University, Salalah 211, Oman; mzghaibeh@du.edu.om

² Laboratoire Analyse, Conception et Commande des Systèmes (LR11ES20), Ecole Nationale d'Ingénieurs de Tunis, Université de Tunis El Manar, Tunis 1002, Tunisia

³ Laboratoire de Génie Mécanique, Ecole Nationale d'Ingénieurs de Monastir, Université de Monastir, Monastir 5019, Tunisia; ikrambenbelgacem@gmail.com

⁴ Research Unit on Study of Industrial Systems and Renewable Energy (ESIER), Université de Monastir, National Engineering School of Monastir, Université de Monastir, Monastir 5019, Tunisia; khiareddine_abla@yahoo.fr

⁵ Energy and Thermal Systems Laboratory, National Engineering School of Monastir, Street Ibn El Jazzar, Monastir 5019, Tunisia; Iskander.Tlili@enim.rnu.tn

* Correspondence: ebarhoumi@du.edu.om; Tel.: +968-98190380

Received: 26 October 2018; Accepted: 4 December 2018; Published: 6 December 2018



Abstract: This paper presents a simple strategy for controlling an interleaved boost converter that is used to reduce the current fluctuations in proton exchange membrane fuel cells, with high impact on the fuel cell lifetime. To keep the output voltage at the desired reference value under the strong fluctuations of the fuel flow rate, fuel supply pressure, and temperature, a neural network controller is developed and implemented using Matlab-Simulink (R2012b, MathWorks limited, London, UK). The advantage of this controller resides in its simplicity, where limited number of tests are carried out using Matlab-Simulink to construct it. To investigate the robustness of the proposed converter and the neural network controller, strong variations of the fuel flow rate, fuel supply pressure, temperature and air supply pressure are applied to both the fuel cell and the neural network controller of the converter. The simulation results show the effectiveness and the robustness of the both the proposed controller and converter to control the load voltage and minimize the current and voltage ripples. As a result of that, fuel cell current oscillations are considerably reduced on the one hand, while on the other hand, the load voltage is stabilized during transient variations of the fuel cell inputs.

Keywords: proton exchange membrane fuel cell; four phases interleaved boost converter; neural network controller

1. Introduction

Fuel cell technologies are becoming used in many industrial applications due to the cleanliness, high reliability and high performance of such electrical generators [1]. During the last decades, many kinds of fuel cells were developed and used. However, the proton exchange membrane fuel cell (PEMFC) has proved to have a higher efficiency when compared to other types of fuel cells [2]. In addition to its long life time, the PEMFC is characterized by its high power density at low operating temperature [3]. Moreover, the PEMFCs have good dynamic responses during instantaneous power demand variation. Nowadays, the PEMFCs are connected to hybrid renewable energy sources with energy storage systems like batteries and super capacitors [4]. Usually, such hybrid systems are used in hybrid electric vehicles to improve the performance of the global system during the peak power

demand transient and instantaneous variation [5]. PEMFCs are used in electrical and hybrid cars such as Toyota, Honda, Hyundai, Nissan and Ford fuel cells cars developed their during the last years [5]. Under no load conditions, a PEMFC cell generates a low direct current voltage, approximately 1 V/cell. Typically, a sufficient number of cells are connected in series to increase the PEMFC voltage. However, the PEMFC voltage is still not enough for high load voltage demands. To increase the PEMFC voltage with the aim to meet the requirements of the load, a boost DC-DC converter is used to control the flow of the power from the PEMFC to the load and to prevent the PEMFC from overloading [6,7]. The power converters associated with fuel cells should have specific characteristics. Undeniably, the fuel cell is very sensitive to low and high frequency currents created by power electronic converters and loads [8]. Low and high frequency components of currents reduce the PEMFC output power and decrease the durability of the membranes [9]. To improve the lifespan of PEMFCs, many solutions were proposed to reduce the ripple and harmonic components of the current, as reported in [10–12]. One of the various proposed power converters is the multiphasing or interleaved DC-DC boost converter [13]. This converter consists of a parallel connection of simple boost converters, hence, it allows to minimize the ripple and harmonic contents of the voltage and current. The control of a multiphase interleaved boost DC-DC converter for classic voltage sources, i.e., batteries, usually consists of an inner current control loop and outer voltage control loop [14]. This kind of control has shown good performance in regulating the output voltage [15,16]. However, the control of the interleaved boost converter associated with PEMFC should follow different strategies due the non-linear characteristics of the PEMFC [17,18]. Indeed, any increase of the load current increases the PEMFC current. Hence, the PEMFC voltage decreases and the desired load voltage becomes unachievable [19]. The control of a superconducting magnetic energy storage (SMES) system for hybrid energy storage systems using fuel cells allows generating or absorbing load pulses to protect the fuel cell [20]. The proposed method shows good efficiency to control the variability of the load demand by using the load following control for auxiliary energy source. However, it could not be applied in a system using only a fuel cell. A boost converter working in differential and common mode is analysed in [21]. In differential mode, the converter allows one to regulate the ac output voltage. The common mode is adopted for current ripple reduction. The method is based on the use of repetitive controllers. Furthermore, a buck-boost DC-DC converter having a regulated output voltage was presented in [22]. The buck-boost was used as a second converter after a single-ended primary-inductance converter (SEPIC). The controller was designed in a way to have a regulated output voltage. In [23], a three phase interleaved boost converter was proposed and analyzed. The simulation of the average model of the converter has shown a good performance in reducing the current ripple. On the other side of the fuel cell, the temperature should be stabilized in optimal range using appropriate techniques of control. Indeed, a control of temperature allows a 10% increasing of the output power [24]. In [25], a real time optimization strategy was adopted to find the optimal value of the fuel flow rate. A maximum power point technique based on neural network was developed for the control of three phase interleaved boost converter. This method allowed to extract the maximum power from the fuel cell system under different temperature conditions. The voltage across the load was not regulated at reference value [26]. The sliding mode control of a coupled interleaved boost converter associated with a PEMFC system allows reducing the current ripples and regulating the load voltage at the presence of variable load. However, the adapted controller did not show the effect of the source conditions variation, i.e., temperature, pressure on the regulated output voltage [27].

In this paper, the objectives of the proposed converter and its controller are the mitigation of the load pulses as well as the regulation of the output voltage. In comparison with the method and results presented in [21], the proposed solution consists of the generating the required duty cycle to regulate the output voltage. The proposed PWM allows minimizing the ripple of current for all output voltage. This work adopts a non-conventional control technique based on the use of a neural network to control the interleaved boost DC-DC converter associated to the PEMFC. The remaining of the paper is organized as follows. Section 2 is dedicated to the presentation and the modelling of the

PEMFC. In Section 3, the interleaved boost DC-DC converter is presented, analysed and simulated using Matlab-Simulink. In Section 4, the impact of external parameters on both load voltage and PEMFC voltage is quantified through simulations. The design of the new controller of the interleaved boost converter is presented in Section 5. Simulations results of the control of PEMFC-boost converter are presented and analysed in Section 6. Finally, conclusions and recommendations are summarized in Section 7.

2. Fuel Cell Modeling

In this paper, the considered model was developed in [1,2]. The differences in equations of the model are summarized in the following expressions. The output voltage of an elementary cell is given by [1]:

$$V_{Cell} = E_0 - \Delta V \quad (1)$$

where E_0 is the reversible voltage of the cell, called also the thermodynamic potential of the cell. This voltage is given by [2]:

$$E_0 = 1.229 - 0.85 \times 10^{-3} \times (T - 298.15) + 4.31 \times 10^{-5} \times T \times [\log(P_{H_2}) + 0.5 \log(P_{O_2})] \quad (2)$$

The voltage drop in the PEMC due to the electrical and chemical factors is the sum of three voltages: activation voltage, ohmic voltage and the concentration voltage. Hence, the cell voltage is expressed as [1,2]:

$$V_{Cell} = E_0 - V_{act} - V_{ohm} - V_{conc} \quad (3)$$

The activation losses are described by the activation overvoltage, V_{act} [1]:

$$V_{act} = -(\xi_1 + \xi_2 T + \xi_3 T \log(c_{O_2}) + \xi_4 T \log(i_{FC})) \quad (4)$$

The term i_{FC} is the fuel cell stack current. ξ_1 , ξ_3 and ξ_4 are constants, given respectively by [1,2]:

$$\begin{aligned} \xi_1 &= -0.948 \\ \xi_3 &= 7.6 \times 10^{-3} \\ \xi_4 &= -1.93 \times 10^{-4} \end{aligned}$$

The parameter ξ_2 depends to the membrane area and the concentration of hydrogen [1,2].

$$\xi_2 = 0.00286 + 0.0002 \log(A_{cell}) + 4.3 \times 10^{-5} \log(C_{H_2}) \quad (5)$$

The oxygen concentration in the catalytic interface of the cathode is expressed by [1,2]:

$$c_{O_2} = \frac{P_{O_2}}{5.08 \times 10^6 \exp\left(-\frac{498}{T}\right)} \quad (6)$$

where P_{O_2} is the pressure of oxygen in the catalytic interface of the cathode.

The ohmic voltage is given by [2]:

$$V_{ohm} = i_{FC} R_{ohm} = i_{FC} (R_{mem} + R_e) \quad (7)$$

where R_{mem} is the equivalent resistance of the membrane expressed as in [1]:

$$R_{mem} = \frac{\rho_{mem} l}{A} \quad (8)$$

where l and A are respectively the thickness and the area of the membrane. The resistivity of the membrane, ρ_{mem} , is given by [2]:

$$\rho_{mem} = 186 \left[1 + 0.03 \left(\frac{i_{FC}}{A} \right) + 0.062 \left(\frac{T}{303} \right)^2 \left(\frac{i_{FC}}{A} \right)^{2.5} \right] / \left[\Psi - 0.634 - 3 \left(\frac{i_{FC}}{A} \right) \right] \cdot \exp \left[4.18 \left(\frac{T-303}{T} \right) \right] \quad (9)$$

As a result of the concentration of reactants consumed in the reaction, a voltage called concentration overvoltage is defined and given by [2]:

$$V_{conc} = -B \log \left(1 - \frac{\left(\frac{i_{FC}}{A} \right)}{\left(\frac{i_{FC}}{A} \right)_{max}} \right) \quad (10)$$

The factor *B* is a parameter that depends to the fuel cell. The PEMFC is selected based on the maximum power required by the DC bus, which is about 1 kW. The required voltage on the DC bus is 60 V. Then, the PEMFC having the parameters given in Table 1 is selected.

Table 1. PEMFC Electrical Parameters.

Parameter	Value
Stack rating voltage (V)	24
Power (kW)	1.26
Stack rating Current (A)	52
Maximum Current (A)	100
Maximum voltage (V)	42
Number of Cells	42
Nominal stack Efficiency	46%
Time constant	1 ms

3. Interleaved Boost Converter

The classic boost converter used to step up the voltage is shown in Figure 1. An insulated gate bipolar transistor (IGBT), inductor, capacitor and a diode, essentially compose the boost converter. The output voltage is controlled through the pulse width modulation (PWM) system.

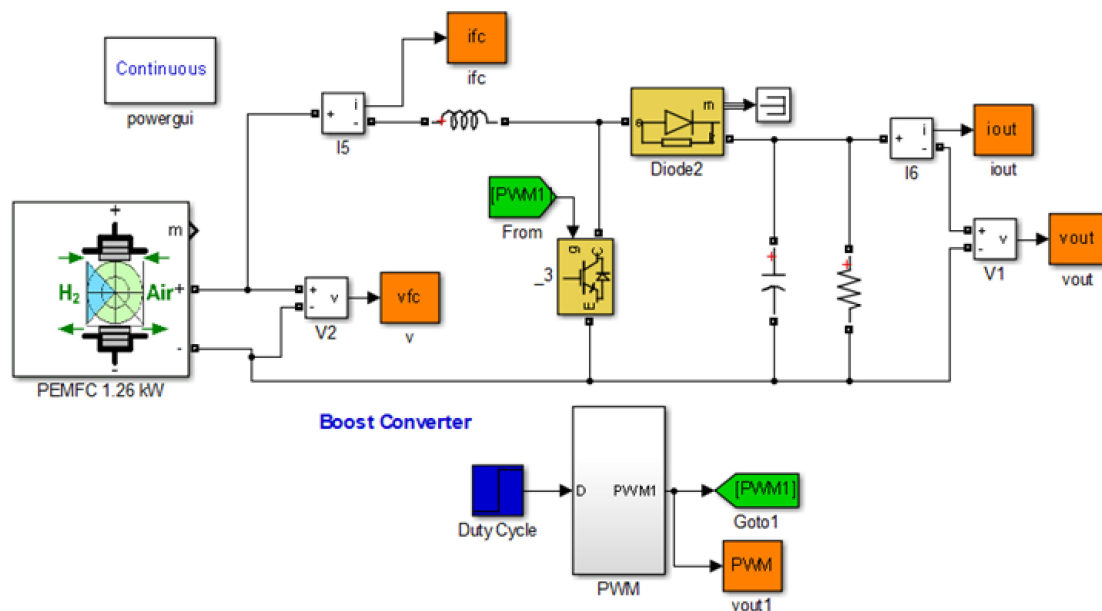


Figure 1. Fuel Cell-Boost Converter System.

A constant signal equal to the duty cycle is compared to the carrier wave to generate the PWM signal to control the IGBT. During DT , the switch is closed and the diode is reverse biased. Accordingly, the variation of the inductor current is given by [6]:

$$(\Delta i_L)_{Closed} = \frac{V_{Load}DT}{L} \quad (11)$$

When the switch is opened, the diode becomes forward biased to ensure a path for the current. Thus, the variation of the inductor current in $(1 - D)T$ is given by [6]:

$$(\Delta i_L)_{Opened} = \frac{(V_{Stack} - V_{Load})(1 - D)T}{L} \quad (12)$$

The average change current in the inductor is equal to zero. Therefore, the load voltage is expressed as follows [8]:

$$V_{Load} = \frac{1}{1 - D} V_{Stack} \quad (13)$$

The maximum voltage of the PEMFC is 42 V. A boost converter is suitable to step up the voltage to reach the load voltage of 60 V. The inductor is selected to minimize the load current ripples to less than 0.5 A. The capacitor is sized to reduce the load voltage to less than 5 V. For a switching frequency and a duty cycle of 25 kHz and 0.5 respectively, the inductor and capacitor values are calculated. The boost converter parameters are summarized in Table 2. The fuel cell boost converter system is simulated in Matlab-Simulink as shown in Figure 1. The aim of this simulation is to evaluate the ripple of the load voltage, stack voltage, load current and stack current. The simulation results are presented in Figure 2a,b.

Table 2. Boost Converter parameters.

Parameter	Symbol	Value
Inductance (mH)	L	1
Capacitance (μ F)	C	50
Input Voltage (V)	V_{Stack}	—
Load resistance (Ω)	R	10
Duty Cycle	D	0.5
Frequency (kHz)	f	25

Figure 2a shows a load current ripple equals to 0.6 A. The load voltage oscillation is equal to 6 V as shown in Figure 2b. In the design of DC/DC converters, reducing the voltage and current oscillations leads to the selection of the best values of the inductor and the capacitor based on the following equations [6]:

$$L_{min} = \frac{D(1 - D)^2 R}{2f} \quad (14)$$

$$C_{min} = \frac{D}{R \left(\frac{\Delta V_{Load}}{V_{Load}} \right) f} \quad (15)$$

To minimize the inductor current ripple and the output voltage ripple to the desired values, the inductor and capacitor must be resized according to Equations (14) and (15). Normally, the major problem exists due to the size, weight and cost of high power inductor and capacitor.

Indeed, using high power inductor and capacitor will significantly increase the weight of the DC/DC converter. However, it is crucial to minimize the ripple and harmonic content of the current in the circuit in order to protect the fuel cell as well as to increase the life time of other components. Another solution was proposed to reduce the ripple current and harmonics is based on the use of what is called an interleaved power converter.

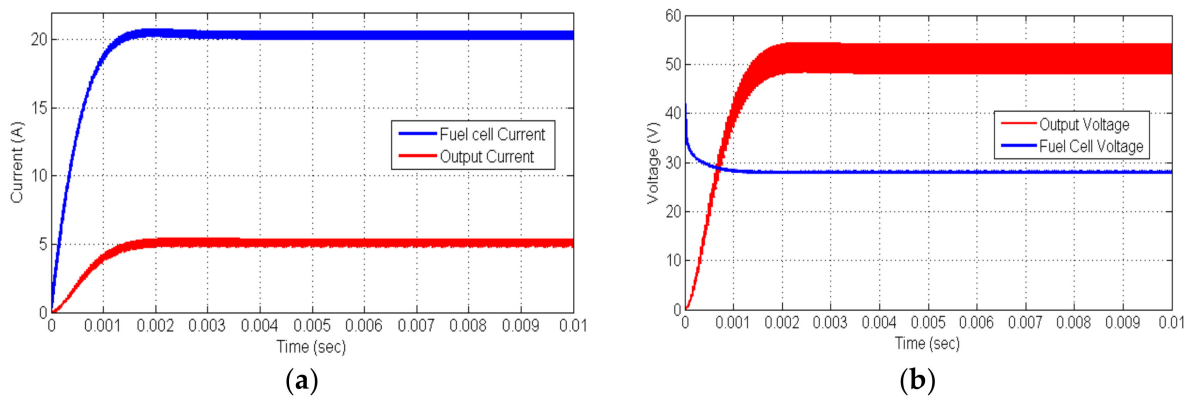


Figure 2. (a) Variation of currents; (b) Variation of voltages.

Simulation of the Four Phases Interleaved Boost Converter

Interleaved converters, also called multiphase, are used to minimize the voltage and current ripples using the same filter components [6]. Therefore, using such interleaved converters allows reducing the size of filter components. The proposed interleaved boost converter is shown in Figure 3. The new boost converter is formed by a parallel combination of four sets of diodes, switches and inductors connected to a common capacitor and load. The PWM signals for the control of the four IGBTs is based on the PWM signal generated to control the first IGBT. Each IGBT control is shifted by a delay time equal to the fourth of the period. For a duty cycle of 0.25, the commutation sequence of the IGBTs is given as follows:

$$\begin{cases} 0 \leq t \leq \frac{T}{4} : IGBT_1 \\ \frac{T}{4} \leq t \leq \frac{T}{2} : IGBT_2 \\ \frac{T}{2} \leq t \leq \frac{3T}{4} : IGBT_3 \\ \frac{3T}{4} \leq t \leq T : IGBT_4 \end{cases} \quad (16)$$

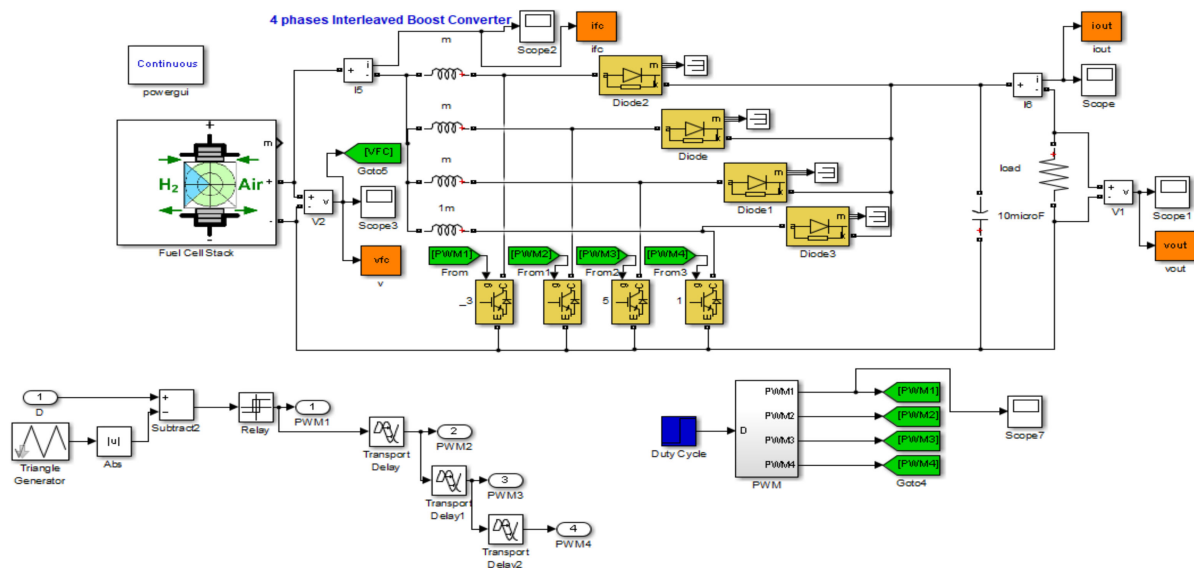


Figure 3. Interleaved Boost Converter and PWM simulation under Matlab-Simulink.

For a duty cycle of 20%, the four PWM signals are shown in Figure 4. The IGBTs are operating at 90° out of phase producing currents that are 90° out of phase. The load current is the sum of the four inductors current. Hence, the resultant load current has a smaller ripple and a frequency which is four

times larger than that of the load current of the single phase boost converter. Figure 3 shows the four phases boost converter and the PWM control for the four IGBTs implemented in Matlab-Simulink.

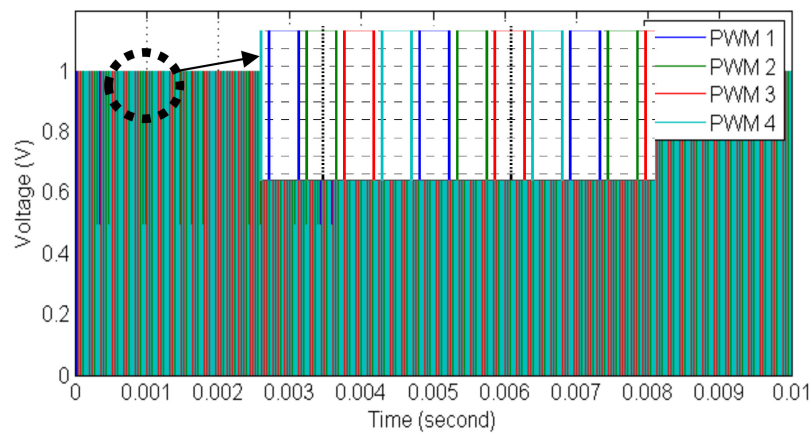


Figure 4. PWM control signals for duty cycle equal to 0.2.

Figure 5a shows the variation of the stack current and electrical current in the load. It is clear in the figure that the current oscillations are reduced to less than 0.2 A. Moreover, the variation in current generated from the PEMFC is reduced. Therefore, the stack current is perfectly smoothed. This allows to increase the life time of the PEMFC. Figure 5b shows the voltage waveforms. Using the proposed four phases interleaved boost converter allows decreasing the load voltage ripple to less than 2 V. Moreover, the PEMFC voltage ripple is decreased considerably.

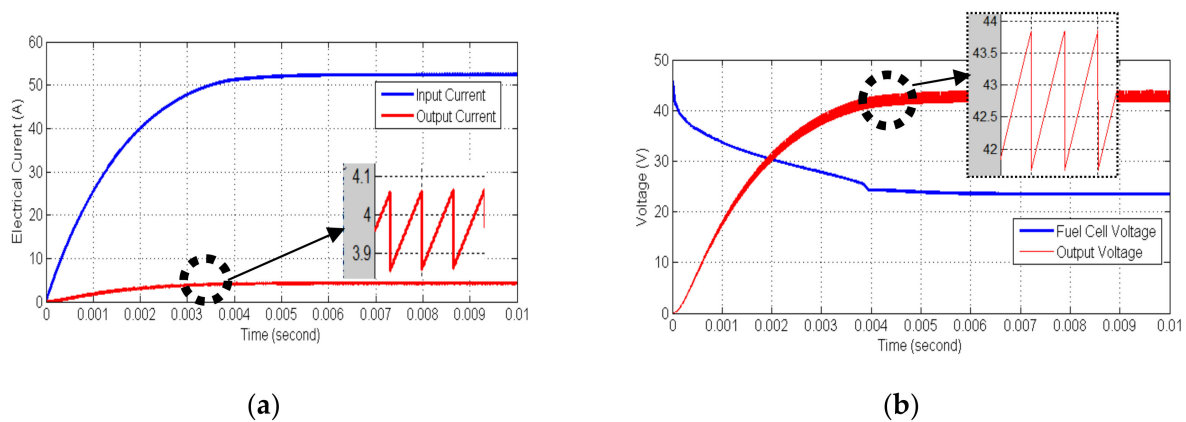


Figure 5. (a) Currents for duty cycle 0.5, (b) Voltages for duty cycle 0.5.

4. Impact of External Parameters on the Output Voltage

To control the PEMFC voltage, it is required to supervise the inputs parameters of the fuel cell. Basically, the stack voltage depends to the pressure and flow rate of the fuel and the air supply. On the other hand, static characteristics show that the temperature of working environment has a strong effect on the PEMFC voltage. This section concerns the dynamic simulation of the fuel cell when varying different variables such as the fuel flow rate, the pressure, the air supply pressure, and the temperature of working environment. Hence, some simulations were carried out in the Matlab-Simulink environment to show the effect of the variation of the physical inputs on the load and PEMFC voltage. In this simulation the duty cycle is fixed at 0.5. Figure 6a shows the variation of the output voltage under temperature variation in three stages. As shown, the temperature has a strong effect on the output voltage of the fuel cell and the load voltage. Evidently, for a temperature equal to 273 K, the PEMFC voltage and the load voltage are equal to 18 V and 35 V, respectively.

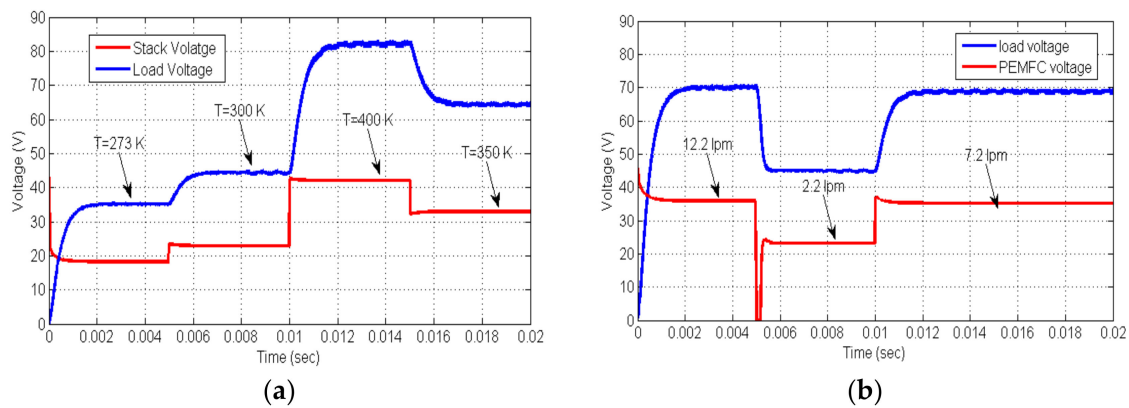


Figure 6. PEMFC and load voltages for (a) temperature variation (b) variation of fuel flow rate.

The figure illustrates that an increase by 23 K increases the load voltage to 44 V. At 0.01 s a strong temperature increment of 100 K is applied. As a result of that, the load voltage has stepped up to more than 80 V. Reducing the temperature to 350 K, allows stepping down the load voltage to 65.02 V. Both PEMFC voltage and load voltage vary with the stack temperature. To maintain the load voltage to a desired value, it is required to update the duty cycle each time. The variation of the load voltage and PEMFC voltage for different fuel flow rate and constant duty cycle is presented in Figure 6b. The simulation results show the high effect of the fuel flow rate on both PEMFC voltage and load voltage. For a fuel flow rate equal to 12.2 lpm, the load voltage is about 70 V for a fixed duty cycle equal to 0.5. Due to a decline of fuel flow rate to a value of 2.2 lpm, the load voltage decreases to 45 V. In recapitulation, the load voltage and the PEMFC voltage are both dependent on the input variables of the PEMFC.

Figure 7a,b show the variation of the PEMFC and load voltages versus time for different fuel flow rate and different fuel supply pressure respectively. It is clear from these results that the PEMFC voltage is dependent on the fuel supply pressure and fuel flow rate. However, this dependence is non-linear, as shown. Undeniably, for 7 lpm as fuel flow rate, the PEMFC voltage is 15 V. An increase by 3 lpm in the fuel flow rate allows to increase the voltage to 20 V. However increasing the fuel flow rate from 17 lpm to 20 lpm increases the voltage by almost 1 V. This result confirms the nonlinearity of the variation of the voltage versus the variation of the fuel flow rate. The same comments are deduced from the results given in Figure 7b.

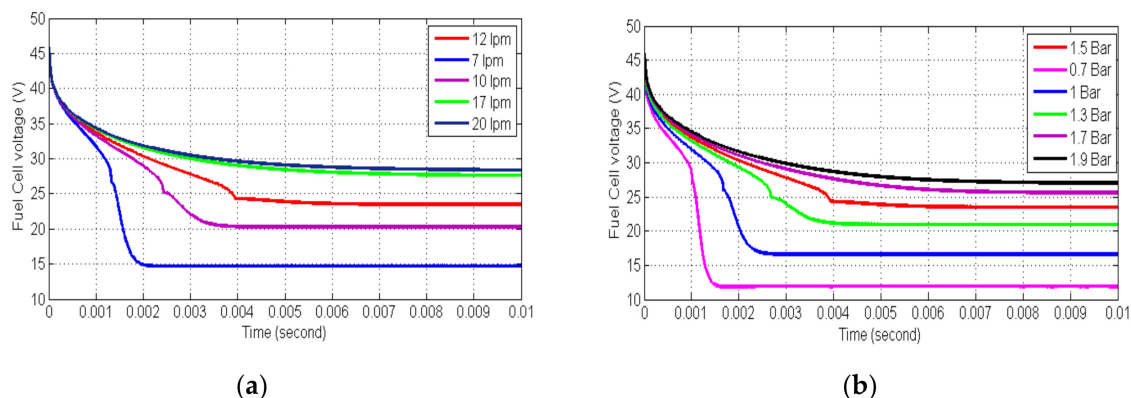


Figure 7. PEMFC voltage for: (a) different fuel flow rate; (b) different fuel supply pressure.

5. Neural Network Regulation

As presented in the last section, the load voltage depends on external variables like the temperature, fuel supply pressure, fuel flow rate and other PEMFC input variables. Therefore, any variation of the input variables affects considerably the PEMFC voltage and consequently the load

voltage. However, in all industrial applications, especially the hybrid or electric vehicle, it is required to regulate the continuous bus. As a solution, the duty cycle must be updated to keep the load voltage to a desired output. Usually the proportional integral derivative (PID) controller and the proportional integral (PI) controller are used to adjust the duty cycle. However, due to the multiple inputs of the PEMFC like the hydrogen supply pressure, hydrogen flow rate, temperature, air supply pressure and air flow rate, it is compulsory to use a neural network to control the duty cycle.

The artificial neural network (ANN) was developed and recognized as efficient approach for the control of nonlinear systems [28]. During the last decades, the ANN contributed to the improvement of industrial applications where the systems presented complexity in control and modeling [29]. The ANN was used to control the power converters in many cases [29,30]. Due to the multiple inputs of the fuel cell, the ANN is preferred in this case to control power converter by generating the duty cycle. Then, it seems clear that the inputs of the ANN will be the same inputs of the fuel cell in addition to the desired load voltage. The ANN controller will calculate the duty cycle according the fuel cell inputs and the desired load voltage. To achieve this objective, many tests were carried out in aim to prepare a database for the ANN.

The methodology consists on running the simulation for different values of duty cycle while keeping the same values of the inputs of the PEMFC and measuring the output voltage each time. The test is repeated for different values of the temperature, fuel supply pressure, fuel flow rate and air supply pressure. All these parameters can change at any time due to wrong manipulation or any fault in the external equipment used with the fuel cell such as the fuel compressor or the air-conditioning system. Figure 8a shows the variation of the duty cycle versus the load voltage for different values of the temperature. The data extracted from this graph formulate the first data to build the ANN. The inputs of the ANN are fuel flow rate, airflow rate, temperature, fuel supply pressure, air supply pressure and desired load voltage. The output of the ANN is the duty cycle. According to the values of the inputs, the ANN controller calculates the required duty cycle. To obtain a load voltage equal to 80 V, the duty cycle should be adjusted to 0.42 if the temperature of the PEMFC is about 400 K. To get the same load voltage for a temperature equal to 273 K, a duty cycle of 0.8 should be applied to the power converter. Therefore, it is required to adjust the duty cycle according to the desired load voltage and the temperature of the PEMFC. Figure 8b shows the variation of the duty cycle versus the load voltage for different values of the fuel flow rate. It is clear in Figure 8b below that for lower load voltage, the fuel flow rate does not have a strong effect on the duty cycle value. For the voltages less than 60 V, the graphs are superposed. However, for load voltage more than 65 V, the effect of the fuel flow rate is observed. Then, for higher fuel flow rate, the desired load voltage is obtained with smallest duty cycle. These samples of data are introduced to build the ANN controller.

Figure 8c shows the variation of the duty cycle versus the load voltage for three different values of the fuel supply pressure. The load voltage values are obtained by running the simulation for each value of the pressure and varying the duty cycle from 0.1 to 0.9. The duty cycle is dependent on the load voltage and the fuel supply pressure. Figure 8d shows the variation of the duty cycle versus the load voltage for different values of the air supply pressure. The air supply pressure can be affected by external air parameters. The variation of the air supply pressure affects the fuel cell output voltage. Hence, it is required to study the effect of this parameter on the load voltage. The results presented in Figure 8d below show a non-linearity of the variation of the duty cycle versus the load voltage for each value of the air supply pressure. These samples of results obtained from simulations will be considered in the ANN design. In addition to other PEMFC inputs, the duty cycle must be updated according to the air supply pressure.

To design the ANN controller, all the data corresponding to the variation of the duty cycle versus the load voltage for different values of PEMFC inputs are considered. The ANN is trained with the back propagation neural network (BPNN) method. The BPNN has been adopted for the control of power converters and electrical machines in [28]. The method has been proved its efficiency. To measure the error during the training of the ANN controller, the mean squared error method is adopted. As shown

in Figure 9, the best training performance, achieved at epoch 2000, is 4.11×10^{-7} . After training, the ANN controller is ready to be tested. In next section, the ANN connected to the fuel cell and the power converter is simulated to test the robustness of the developed control.

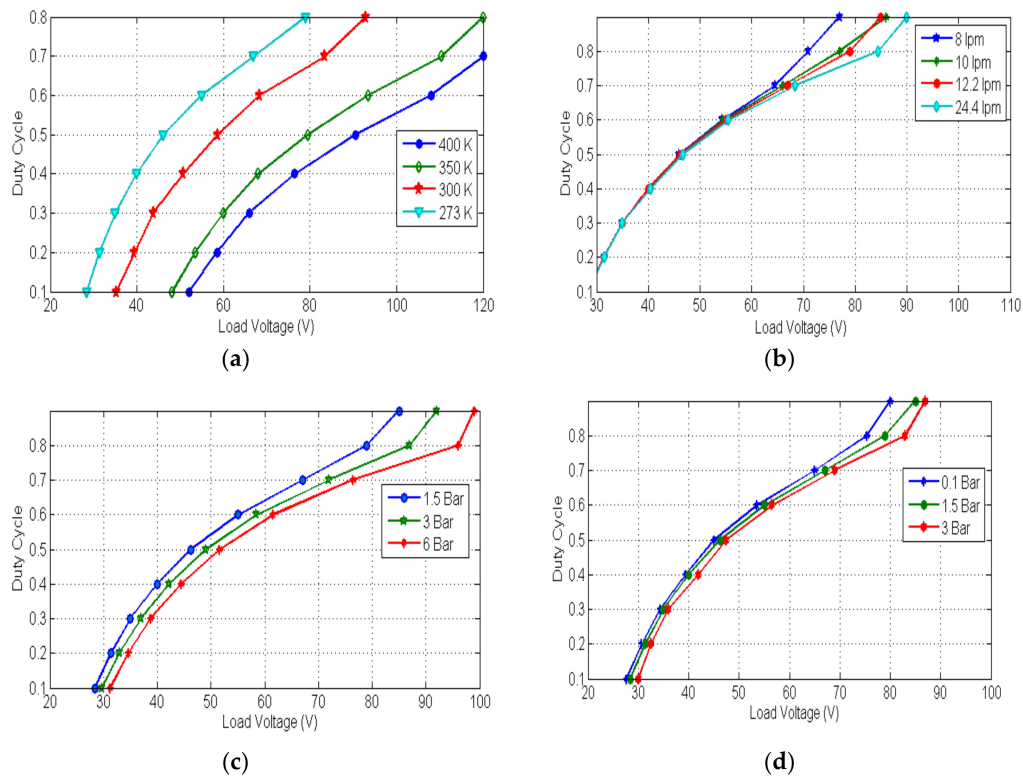


Figure 8. Duty cycle for: (a) different temperature values, (b) different values of the fuel flow rate, (c) different values of the fuel supply pressure, (d) different values of the air supply pressure.

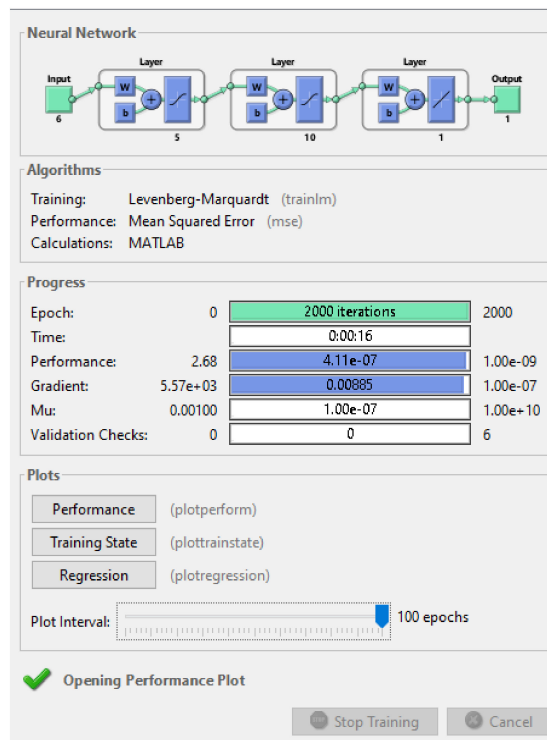


Figure 9. Implementation of the Artificial Neural Network under the Matlab-Simulink.

6. Implementation of the Neural Network Controller

6.1. Effect of the Load Impedance Variation

Figure 10 shows the ANN controller implemented in Matlab-Simulink and associated with the interleaved boost converter and the PEMFC. The inputs of the ANN controller are the same inputs of the PEMFC in addition to the desired load voltage. Thus, any variation of the PEMFC inputs will affect the output of the ANN controller. Figure 11 shows the response of the load voltage to the variation of the load impedance. For all selected values of the load resistance, we can satisfactorily obtain the desired load voltage of 60 V. In the case of decreasing the load resistance from 15 Ω to 10 Ω , an overshoot of 26% is observed. The settling time is about 0.002 s. However, decreasing the load resistance from 10 Ω to 5 Ω will increase the overshoot and the settling time to 50% and 0.0036 s respectively. Overall, the reference voltage is reached and the regulator presents good robustness to regulate the load voltage.

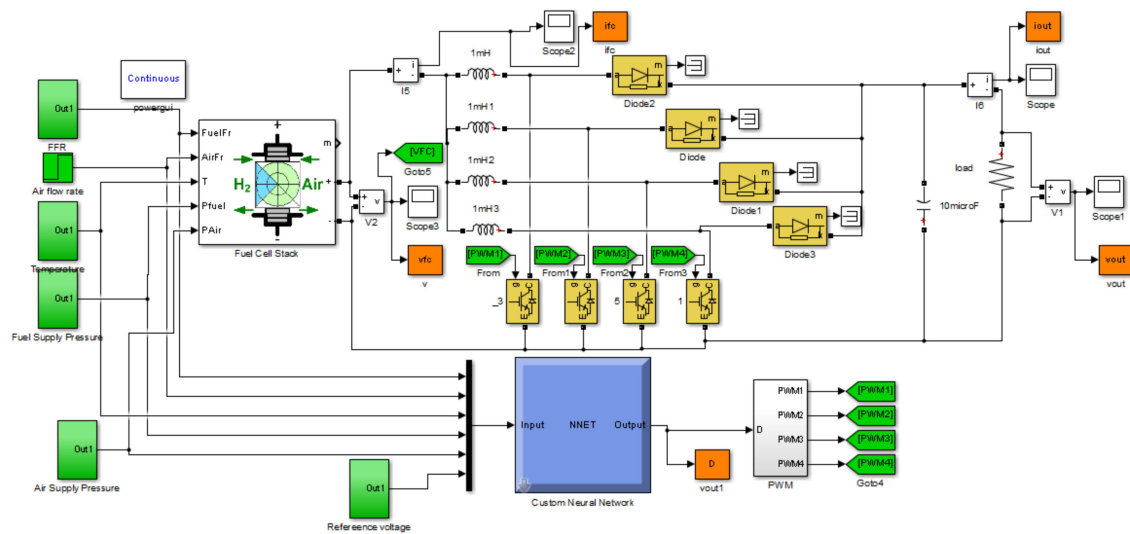


Figure 10. Fuel Cell- Boost Converter System and Neural Network Controller.

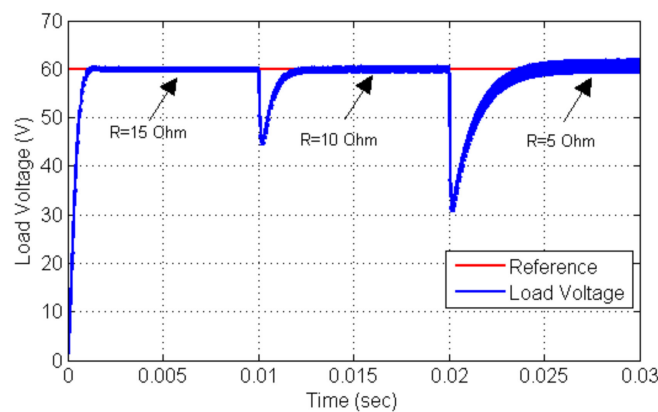


Figure 11. Output voltage response to the variation of the load resistance for desired output of 60 V.

6.2. Effect of the Temperature Variation

To study the effect of the temperature variation on the load voltage, the temperature is increased from 273 K to 300 K at 0.005 s in first time. At 0.01 s an increment of 100 K is applied to the temperature input. Finally, the temperature is reduced to 350 K at 0.015 s. the temperature variation is shown in Figure 12a. The load voltage reference is set to 60 V. Figure 12b shows the variation of the duty cycle according to the variation of the temperature. Therefore, any increase of the temperature corresponds to a decrease of the duty cycle. Consequently, the ANN controller calculated to an optimal duty cycle of 60 V as load voltage.

The dynamic responses of the load voltage and the PEMFC voltage are presented in Figure 12c. The PEMFC voltage varies according to any change of the temperature. However, the load voltage is kept at the desired voltage. This is due to the perfect variation of the duty cycle according to any variation of the PEMFC inputs. An overshoots of 25% and 41% are observed at 0.005 s and 0.01 s respectively. These overshoots are satisfactorily attenuated. The dynamic responses of the PEMFC and load currents presented in Figure 12d show the strong variation of the PEMFC current due the variation of the PEMFC voltage. The load current is kept constant. The simulation results show the efficiency of the ANN controller in regulating the load voltage under strong variation of the PEMFC temperature.

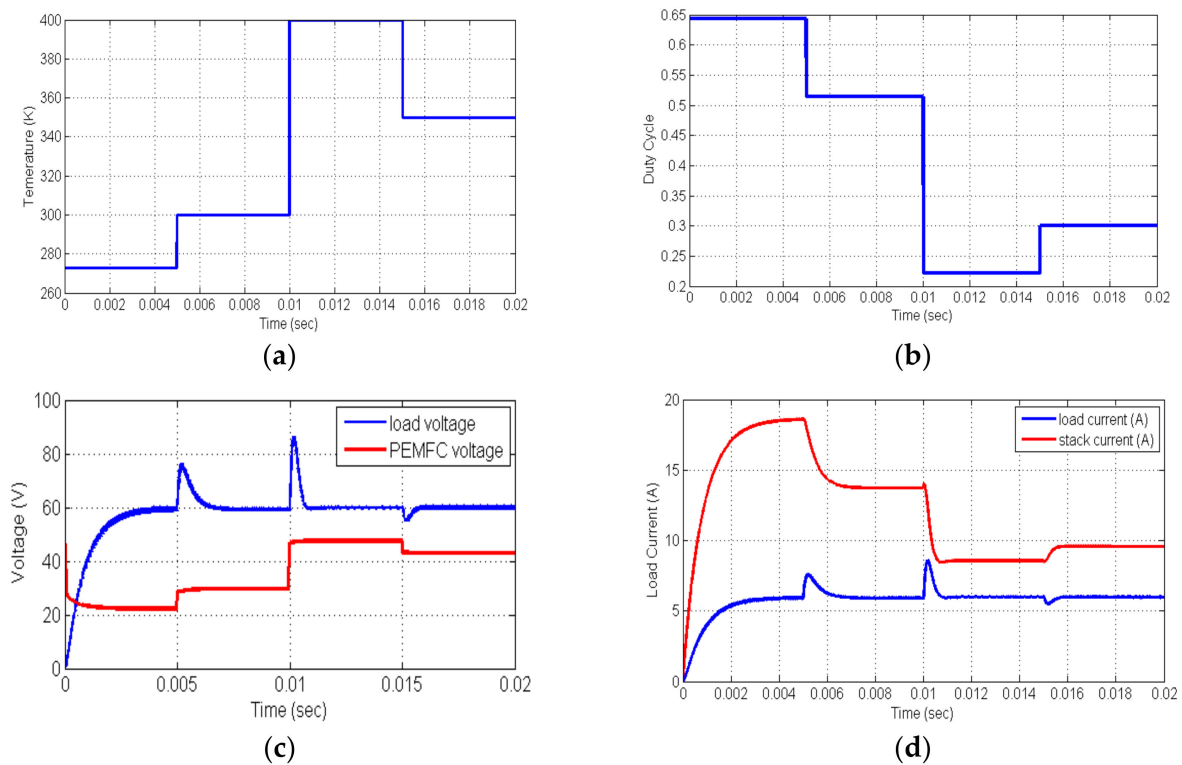


Figure 12. (a) Temperature variation, (b) Variation of the duty cycle, (c) voltage variation, (d) current variation.

6.3. Effect of the Fuel Flow Rate

The nominal value of hydrogen flow rate is about 12.2 lpm. However, this parameter can be influenced at any time due to any fault in the compressor system. To test the response of the system when varying the fuel flow rate, we apply the increments shown in Figure 13a to the PEMFC and the ANN controller. The result presented in Figure 13b shows the variation of the duty cycle according to the variation of the fuel flow rate. Here, the ANN controller proves its robustness under different fuel flow rates. Figure 13c shows that the load voltage is kept to the desired voltage.

Figure 13d shows the variation of the currents in both PEMFC and load. The PEMFC voltage has increased and decreased due to the variation of the fuel flow rate value. Even though the PEMFC output current has increased and decreased, the load current and voltage are retained at the same value. Thus, this test shows the efficiency of the ANN face to fuel flow rate variation.

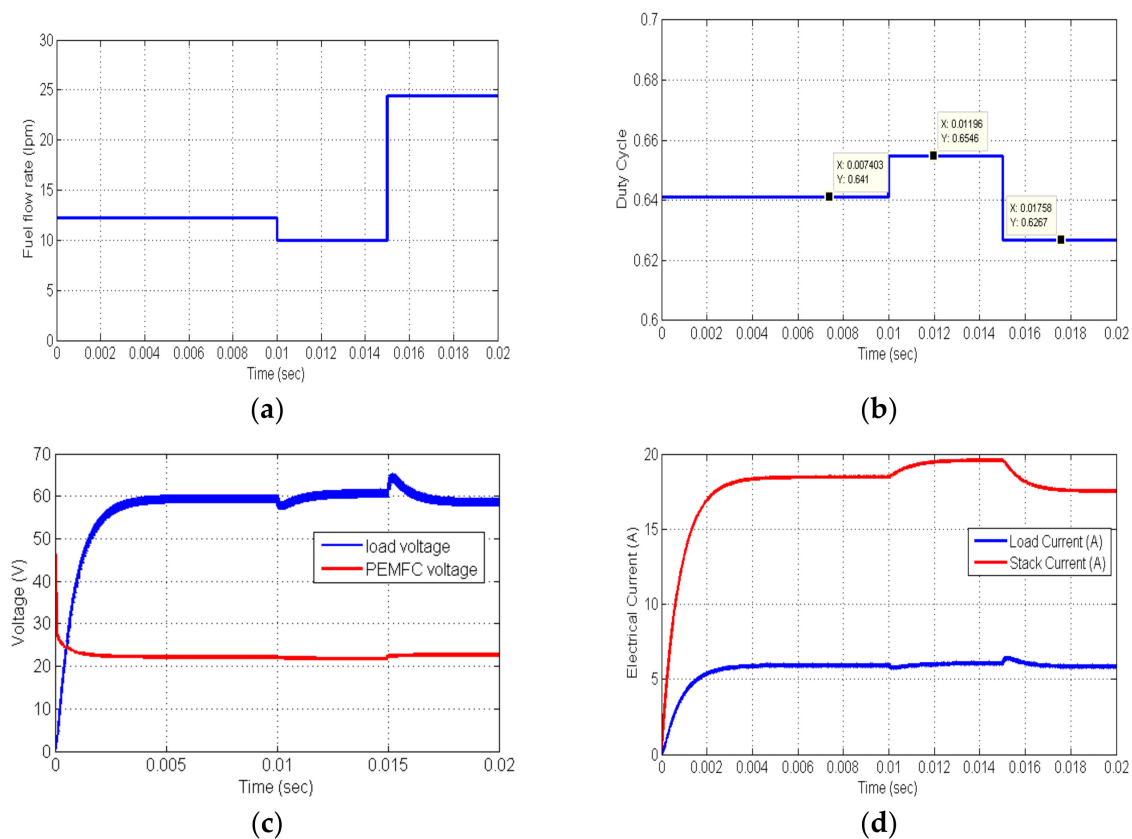


Figure 13. (a) Variation of the fuel flow rate, (b) Variation of the duty cycle, (c) voltage variation, (d) current variation.

6.4. Variation of the Fuel Supply Pressure

Fuel supply pressure drops and increases are terms used to describe the reduction and the increase in the fuel pressure due to the compressor operation. Usually, a properly designed compressor system used for hydrogen supply to the PEMFC must have a constant pressure. However, any fault due to excessive usage can happen and affect the control of the fuel supply pressure. Excessive fuel pressure variation will contribute to poor PEMFC performance and excessive energy losses.

The proposed ANN should take in account the variation of the fuel supply pressure. To test the effect of the fuel supply pressure on the load voltage after implementation of the ANN controller, the increments of Figure 14a are applied to both PEMFC and ANN controller. The simulation results presented in Figure 14b, and Figure 14c show the effectiveness of the ANN controller in updating the duty cycle to regulate the load voltage to 60 V. Figure 14d shows the strong variations of the fuel cell current due to an increase of the fuel supply pressure. The ANN controller adjusts the duty cycle each time to regulate the load voltage.

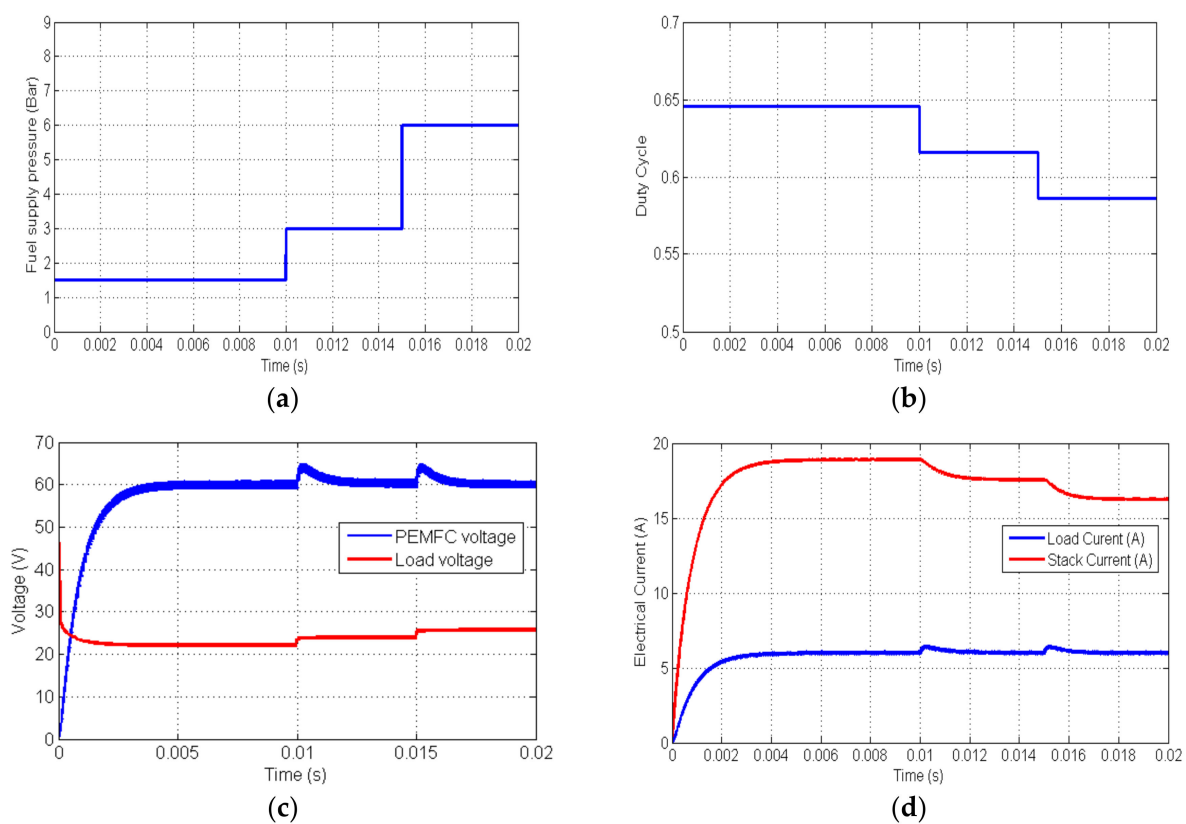


Figure 14. (a) Variation of the fuel supply pressure, (b) Variation of the duty cycle, (c) voltage variation, (d) current variation.

6.5. Variation of the Air Supply Pressure

On the other hand, the air supply pressure is also another factor affecting the performance of the PEMFC in best conditions. Any increase or decrease of the air supply pressure has an effect on the PEMFC voltage. Figure 15a shows the variation of the air supply pressure applied as input for the PEMFC and the ANN controller. Firstly, the air supply pressure is fixed to 1 bar. At the time 0.01 s, the air supply pressure is dropped to 0.1 bar. At the time 0.015 s, an increment of 1.9 bar is applied. Then the final value of the air supply pressure is 2 bar. The output of the ANN controller is presented in Figure 15b. The duty cycle is updated each time to keep the load voltage at the desired value, as shown in Figure 15c, under the variations of the PEMFC voltage resulted from the variation of the air supply pressure.

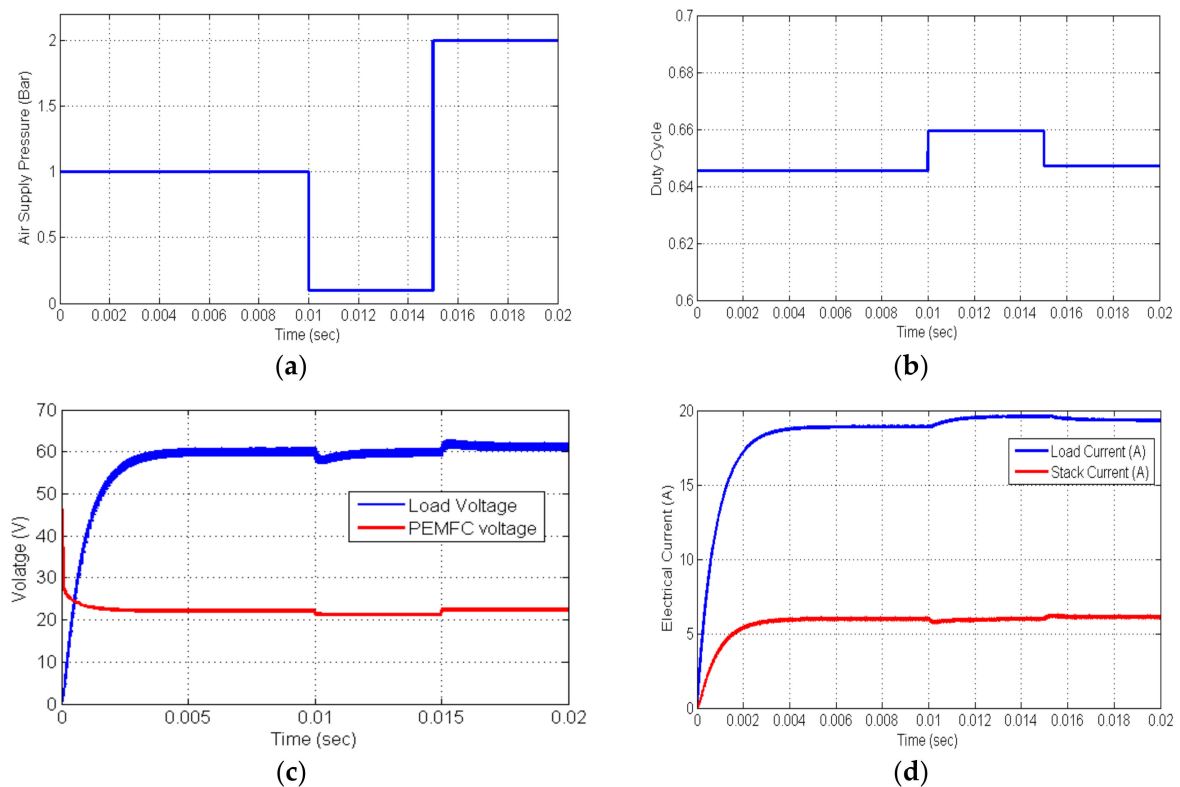


Figure 15. (a) Variation of the air supply pressure, (b) Variation of the duty cycle, (c) voltage variation, (d) current variation.

To test the efficiency of the ANN controller under the variation of the desired output voltage, strong variations of the reference voltage are applied to the controller. The obtained simulation results are shown in Figure 16. The output voltage tracks the reference for different values. Therefore, this result shows a good efficiency of the proposed controller to regulate the output voltage according to the load requirements.

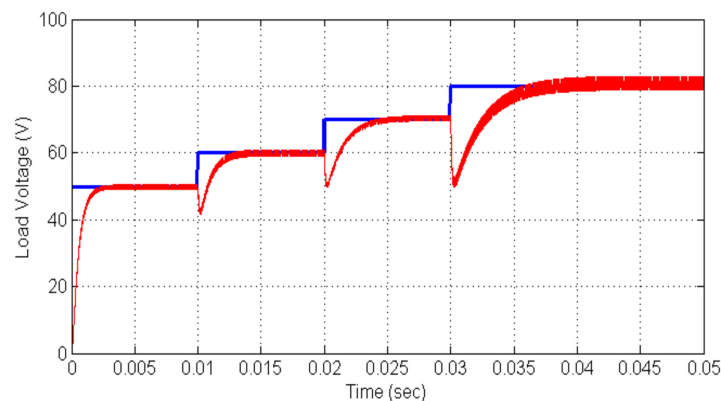


Figure 16. Response of load voltage to reference variation.

The current ripple of the proposed converter-based neural network regulator for PEMFC applications is compared with current ripples obtained with techniques presented in [9,26,27]. The comparison results are listed in Table 3. It is observed that using the proposed converter allows to obtain the lowest current ripples for the PEMFC. A comparative analysis of the proposed controller with proposed techniques in [20,23,25–27] in terms of capability of load voltage regulation in the case of load and source conditions variation is presented in Table 4. It is clear that the proposed controller

in this paper has good capabilities to regulate the load voltage under the variation of the load and source conditions. However, the other proposed techniques present some limits. Indeed, the variations of source conditions were not considered in some analysis.

Table 3. Fuel cell current ripple of the of the proposed converter and techniques presented in [9,26] and [27].

Type of Control	DC Link Voltage	Fuel Cell Current Ripple
Multidevice Interleaved DC/DC Converter for Fuel Cell Hybrid Electric Vehicles [9]	400 V	0.7 A
Maximum Power Point Technique [26]	220 V	0.1 A
Sliding mode control [27]	100 V	0.3 A
Proposed ANN controller for the IBC	60 V	0.01 A

Table 4. Comparison of the proposed controller and proposed techniques in [20,23,25,26] and [27].

Type of Control	Load Voltage Regulation in the Presence of the Variation of					
	Load Impedance	Temperature	Hydrogen Pressure	Hydrogen Flow Rate	Air Pressure	Air Flow Rate
Controlling the SMES hybrid energy storage system [20]	P	NP	NP	NP	NP	NP
Proportional Integral Controller [23]	P	NP	NP	NP	NP	NP
Optimization of the PEMFC Hybrid System [25]	P	NP	NP	P	NP	P
Maximum Power Point Technique [26]	P	P	NP	NP	NP	NP
Sliding mode control [27]	P	NP	NP	NP	NP	NP
Proposed ANN controller	P	P	P	P	P	P

Notes: N.P: Not Performed; P: Performed.

7. Conclusions

To minimize the current and voltage ripples as well as regulating the load voltage, a four phases interleaved boost converter was proposed in this paper. The proposed converter has reduced the ripples of load voltage to less than 2 V. Therefore, using the interleaved boost converter minimized the PEMFC voltage and current ripples. A simple PWM control technique was developed and implemented under Matlab-Simulink for the control of the interleaved boost converter. Simulation results of the open loop control of the interleaved boost converter have shown the incapability to maintain the load voltage at desired value. Indeed, the variation of any external parameter increased or decreased the fuel cell voltage and consequently the load voltage. To overcome this issue, an artificial neural network controller was developed to regulate the load voltage at desired reference. The database used to build this ANN is composed of samples of duty cycle values, load voltage and input parameters of the PEMFC. Compared to other techniques used for the regulation of the fuel supply pressure, fuel flow rate, temperature and air supply pressure based on the use of proportional integral controller to regulate each variable, the proposed strategy allowed to regulate the load voltage with unique controller based on neural network. The simulation results of the interleaved boost converter controlled by the neural network controller show the efficiency and the robustness of the proposed converter to regulate the load voltage as well as minimizing the voltage ripples. The proposed controller showed that using limit number of tests allows to develop efficient ANN controller for the regulation of the load voltage. Therefore, the proposed method will be applied to other PEMFCs having different power range. In future work, a prototype will be developed to test the efficiency of such controllers in real conditions. The behaviour of PEMFC-supercapacitor hybrid system will be investigated to design adequate power converter suitable for such power equipment.

Author Contributions: Conceptualization and methodology, E.M.B. and I.B.B.; Software, A.K. and E.M.B.; Discussion, M.Z.; Review, I.T. and E.M.B.

Funding: This research received no external funding.

Conflicts of Interest: There is no conflict of interest.

References

- Mann, R.F.; Amphlett, J.C.; Hooper, M.A.I.; Jensen, H.M.; Peppley, B.A.; Roberge, P.R. Development and application of a generalised steady-state electrochemical model for a PEM fuel cell. *J. Power Sources* **2000**, *86*, 173–180. [CrossRef]
- Correa, J.M.; Farret, F.A.; Canha, L.N.; Simoes, M.G. An electrochemical-based fuel-cell model suitable for electrical engineering automation approach. *IEEE Trans. Ind. Electron.* **2004**, *51*, 1103–1112. [CrossRef]
- Jin, K.; Ruan, X.; Yang, M.; Xu, M. A hybrid fuel cell power system. *IEEE Trans. Ind. Electron.* **2009**, *56*, 1212–1222. [CrossRef]
- Khiareddine, A.; Salah, C.B.; Rekioua, D.; Mimouni, M.F. Sizing methodology for hybrid photovoltaic/wind/hydrogen/battery integrated to energy management strategy for pumping system. *Energy* **2018**, *153*, 743–762. [CrossRef]
- Fuel Cell Electric Vehicles, Reports Fuel Cell Today. Available online: <http://www.fuelcelltoday.com> (accessed on 15 September 2018).
- Hart, D.W. *Power Electronics*; Mc Graw Hill: New York, NY, USA, 2010; ISSN 978-0-07-338067.
- Rabello, A.L.; Co, M.A.; Simonetti, D.S.L.; Vieira, J.L.F. An isolated DC–DC boost converter using two cascade control loops. In Proceedings of the IEEE International Symposium on Industrial Electronics, Guimaraes, Portugal, 7–11 July 1997; Volume 2, pp. 452–456.
- Sundar, G.; Karthick, N.; Reddy, S.R. High step-up DC–DC converter for ac photovoltaic module with MPPT control. *J. Electr. Eng.* **2014**, *65*, 248–253. [CrossRef]
- Hegazy, O.; van Mierlo, J.; Lataire, P. Analysis, Modeling, and Implementation of a Multidevice Interleaved DC/DC Converter for Fuel Cell Hybrid Electric Vehicles. *IEEE Trans. Power Electron.* **2012**, *27*, 2237–2245. [CrossRef]
- Lee, S.; Park, J.; Choi, S. A three-phase current-fed push–pull DC–DC converter with active clamp for fuel cell applications. *IEEE Trans. Power Electron.* **2011**, *26*, 2266–2277. [CrossRef]
- Lim, T.C.; Williams, B.W.; Finney, S.J.; Zhang, H.B.; Croser, C. Energy recovery snubber circuit for a dc-dc push–pull converter. *IET Trans. Power Electron.* **2012**, *5*, 863–872. [CrossRef]
- Whitaker, B.; Martin, D.; Cilio, E. Extending the operational limits of the push-pull converter with SiC devices and an active energy recovery clamp circuit. In Proceedings of the 2015 IEEE Applied Power Electronics Conference and Exposition (APEC), Charlotte, NC, USA, 15–19 March 2015; pp. 2023–2038.
- Omkun, S.; Sirisamphanwong, C.; Sukchai, S. A DSP-based interleaved boost DC-DC converter for fuel cell applications. *Int. J. Hydrog. Energy* **2015**, *40*, 6391–6404. [CrossRef]
- Thounthong, P.; Rael, S.; Davat, B. Behaviour of a PEMFC supplying a low voltage static converter. *J. Power Sources* **2006**, *156*, 119–125.
- Saha, S.S. Efficient soft-switched boost converter for fuel cell applications. *Int. J. Hydrog. Energy* **2011**, *36*, 1710–1719. [CrossRef]
- Giaouris, D.; Stergiopoulos, F.; Ziogou, C.; Ipsakis, D.; Banerjee, S.; Zahawi, B.; Pickert, V.; Voutetakis, S.; Papadopoulou, S. Nonlinear stability analysis and a new design methodology for a PEM fuel cell fed DC-DC boost converter. *Int. J. Hydrog. Energy* **2012**, *37*, 18205–18215. [CrossRef]
- Hinaje, M.; Sadli, I.; Martin, J.P.; Thounthong, P.; Rafel, S.; Davat, B. Online humidification diagnosis of a PEMFC using a static DC-DC converter. *Int. J. Hydrog. Energy* **2009**, *34*, 2718–2723. [CrossRef]
- Kirculies, M. Fuel cell power for maritime applications. *Fuel Cells Bull.* **2005**, *2005*, 12–15.
- Thounthong, P.; Davat, B.; Rae, S.; Sethakul, P. Fuel Cell high power applications. *IEEE Trans. Ind. Electron. Mag.* **2009**, *3*, 32–46.
- Bizon, N. Effective mitigation of the load pulses by controlling the battery/SMES hybrid energy storage system. *Appl. Energy* **2018**, *229*, 459–473. [CrossRef]
- Lu, N.; Yang, S.; Tang, Y. Ripple Current Reduction for Fuel-Cell-Powered Single-Phase Uninterruptible Power Supplies. *IEEE Trans. Ind. Electron.* **2017**, *64*, 6607–6617. [CrossRef]

22. Kaouane, M.; Khelifaa, A.B.; Cheritib, A. Regulated output voltage double switch Buck-Boost converter for photovoltaic energy application. *Int. J. Hydrog. Energy* **2016**, *41*, 20847–20857. [[CrossRef](#)]
23. Farhani, S.; Amari, M.; Marzougui, H.; Bacha, F. Analysis, modeling and implementation of an interleaved boost DC-DC converter for fuel cell used in electric vehicle. *Int. J. Hydrog. Energy* **2017**, *42*, 28852–28864. [[CrossRef](#)]
24. Ou, K.; Yuan, W.-W.; Choi, M.; Yang, S.; Kim, Y.-B. Performance increase for an open-cathode PEM fuel cell with humidity and temperature control. *Int. J. Hydrog. Energy* **2017**, *42*, 29852–29862. [[CrossRef](#)]
25. Bizon, N.; Mazare, A.G.; Ionescu, L.M.; Enescu, F.M. Optimization of the Proton Exchange Membrane Fuel Cell Hybrid Power System for Residential Buildings. *Energy Convers. Manag.* **2018**, *163*, 22–37. [[CrossRef](#)]
26. Reddy, K.J.; Sudhakar, N. High Voltage Gain Interleaved Boost Converter with Neural Network Based MPPT Controller for Fuel Cell Based Electric Vehicle Applications. *IEEE Access* **2018**, *6*, 3899–3908. [[CrossRef](#)]
27. Wang, W.Y.; Ding, Y.H.; Ke, X.; Ma, X. Sliding mode control of direct coupled interleaved boost converter for fuel cell. In *IOP Conference Series: Earth and Environmental Science*; Conference 1; IOP Publishing: Bristol, UK, 2017; Volume 100.
28. Barhoumi, E.M.; Ben Salah, B. Modelling and Control of a new Linear Switched Reluctance Motor for Shunting the Railways Channels. *Int. Rev. Model. Simul. (IREMOS)* **2011**, *4*, 2012–2019.
29. Barhoumi, E.M.; Ben Salah, B. New Positioning Control of Stepper Motor using BP Neural Networks. *J. Emerg. Trends Comput. Inf. Sci.* **2011**, *2*, 300–306.
30. Barhoumi, E.M.; Ben Salah, B. Design and Simulation of a new Linear Switched Reluctance Motor for Shunting the Railways Channels. *Int. Rev. Model. Simul. (IREMOS)* **2011**, *3*, 1072–1078.



© 2018 by the authors. Licensee MDPI, Basel, Switzerland. This article is an open access article distributed under the terms and conditions of the Creative Commons Attribution (CC BY) license (<http://creativecommons.org/licenses/by/4.0/>).